A Fully Automatic Estimation of Tear Meniscus Height Using Artificial Intelligence

Shaopan Wang,[1,2] Xin He,[2,3] Jiezhou He,[1] Shuang Li,[2] Yuguang Chen,[1,2] Changsheng Xu,[1,2] Xiang Lin,[4] Jie Kang,[4] Wei Li,[2,4] Zhiming Luo,[1,] and Zuguo Liu[1,2,4,5]

[1]Institute of Artificial Intelligence, Xiamen University, Xiamen, Fujian, China
[2]Xiamen University affiliated Xiamen Eye Center; Fujian Provincial Key Laboratory of Ophthalmology and Visual Science, Fujian Engineering and Research Center of Eye Regenerative Medicine, Eye Institute of Xiamen University, School of Medicine, Xiamen University, Xiamen, Fujian, China
[3]Department of Ophthalmology, the First Affiliated Hospital of Xiamen University, Xiamen University, Xiamen, Fujian, China
[4]Department of Ophthalmology, Xiang'an Hospital of Xiamen University; Xiamen, Fujian, China
[5]Department of Ophthalmology, The First Affiliated Hospital of University of South China, Hengyang, Hunan, China

Correspondence: Zuguo Liu, Eye Institute of Xiamen University, School of Medicine, Xiamen University, Chengyi Building, 4th Floor, 4221-122, South Xiang'an Rd, Xiamen, Fujian 361005, China; zuguoliu@xmu.edu.cn.
Zhiming Luo, Institute of Artificial Intelligence, Xiamen University, 422, Siming South Road, Xiamen, Fujian 361005, China; zhiming.luo@xmu.edu.cn.
Wei Li, Eye Institute of Xiamen University, School of Medicine, Xiamen University. Chengyi Building, 4th Floor, 4221-122, South Xiang'an Rd, Xiamen, Fujian 361005, China; wei1018@xmu.edu.cn.

SW, XH, and JH contributed equally to this work and thus should be considered co-first authors.

Received: March 22, 2023
Accepted: August 22, 2023
Published: October 4, 2023

Citation: Wang S, He X, He J, et al. A fully automatic estimation of tear meniscus height using artificial intelligence. *Invest Ophthalmol Vis Sci.* 2023;64(13):7. https://doi.org/10.1167/iovs.64.13.7

Purpose. Accurate quantification measurement of tear meniscus is vital for the precise diagnosis of dry eye. In current clinical practice, the measurement of tear meniscus height (TMH) relies on doctors' manual operation. This study aims to propose a novel automatic artificial intelligence (AI) system to evaluate TMH.

Methods. A total of 510 photographs obtained by the oculus camera were labeled. Three thousand and five hundred images were finally attained by data enhancement to train the neural network model parameters, and 60 were used to evaluate the model performance in segmenting the cornea and tear meniscus region. One hundred images were used to test generalization ability of the model. We modified a segmentation model of the cornea and the tear meniscus based on the UNet-like network. The output of the segmentation model is followed by a calculation module that calculates and reports the TMH.

Results. Compared with ground truth (GT) manually labeled by clinicians, our modified model achieved a Dice Similarity Coefficient (DSC) and Intersection over union (Iou) of 0.99/0.98 in the corneal segmentation task and 0.92/0.86 for the detection of tear meniscus on the validation set, respectively. On the test set, the TMH automatically measured by our AI system strongly correlates with the results manually calculated by the ophthalmologists.

Conclusions. We developed a fully automated and reliable AI system to obtain TMH. After large-scale clinical testing, our method could be used for dry eye screening in clinical practice.

Keywords: artificial intelligence (AI), tear meniscus height (TMH), dry eye, image analysis

Dry eye is a chronic ocular surface disease caused by multiple factors,[1] such as age, sex, Sjögren syndrome, and visual display terminal syndrome.[2] It has significant morbidity worldwide with incidence rates from 5% to 50%.[3] Dry eye seriously affects the life quality and work efficiency of individuals.[4] Failure to detect the condition at early stage may cause vision loss in severe dry eye. Therefore, a rapid and accurate method for early diagnosis of dry eye is critical. Currently, the clinical diagnosis approaches for dry eye include tear film break-up time, tear secretion, and tear meniscus height (TMH).[5] Among these tests, the tear meniscus examination is simple, easy to perform, and does not rely on invasive testing facilities, such as sodium fluorescein stains and test strips.

Oculus keratograph is a widely used instrument in clinics to measure TMH for indirectly assessing tear secretion in patients.[6] However, this measurement heavily depends on the ophthalmologist's operation, which may lead to instability and deviations in the measurement outcomes. Therefore, a stable, efficient, and objective method for evaluating the TMH needs to be developed urgently.

Motivated by the application of conventional deep-learning neural networks on natural image processes, there has been a recent resurgence of interest in medical images.[7]

Artificial intelligence (AI) systems based on deep learning have dramatically benefited overburdened doctors in medicine, especially in regions where healthcare resources are lagging. In the ophthalmology field, AI systems have been developed to detect keratitis,[8] predict glaucoma incidence and progression using retinal photographs,[9] manage congenital cataract,[10] and even predict cardiovascular risk with retinal images.[11]

In terms of tear meniscus detection, segmentation for optical coherence tomography (OCT) measurements of the lower tear meniscus was performed using deep learning.[12] The main strengths of OCT lie in its noninvasiveness and rapid image acquisition.[5] Furthermore, OCT can offer 3D imaging, which may contribute to improved disease identification and progression monitoring.[13] However, it is challenging to implement in rural hospitals and less-developed areas due to the lack of OCT equipment. In addition, the operation of OCT is more complex and requires high professional proficiency. Image analysis is complex, time-consuming, and operator-dependent.[14] Cheng Wan et al. tried to use deep learning to identify the tear meniscus region and used a fixed scale factor to calculate the TMH,[15] but this method did not take into account the anatomic differences among individuals, which may affect TMH measurements. Therefore, exploring a novel method for automatic and accurate quantification of the tear meniscus is necessary to aid in the diagnosis of dry eye.

In summary, we have devised an AI-based system aimed at computing the height of the tear meniscus in this study. The system takes as input the images captured by an Oculus Keratograph, and its output consists of the segmented tear meniscus region along with the corresponding TMH values computed by our proposed calculation module. These results hold valuable diagnostic implications for clinicians. Notably, the measurement process used by the AI system is entirely automated, thus eliminating the need for manual intervention. To ascertain the feasibility of our approach, we conducted a comparative analysis between the measurements obtained from the AI system and those provided by ophthalmologists. Our findings serve to establish the efficacy of this method, and we anticipate that the development of this system will contribute to enhancing the auxiliary diagnosis and screening of dry eye conditions.

Materials and Methods

Data Preparation and Preprocessing

The data in this study were collected from Xiamen University affiliated Xiamen Eye Center. Images taken through an Oculus device qualify for the inclusion criteria. However, we excluded images that may hinder corneal and eyelid identification due to certain factors, such as eye trauma, tumors in the lower eyelid, blurry photographs, uneven brightness, tear meniscus that are difficult to mark, and so on. Figure 1 also provides representative images that are eligible and noneligible for this study. Our research plan was approved by the Ethical Committee of the School of Medicine of Xiamen University with the approval number XDYX2022004 and followed by the World Medical Association Declaration of Helsinki.

The experienced ophthalmologists were assigned to screen the 623 original pictures to ensure the quality of pictures used to perform model training. They eliminated images of the tear meniscus that were vague, bright, and uneven, and difficult to label with the naked eye. A total of 510 clear red, green, and blue (RGB) images were retrospectively obtained from May 2021 to March 2022. The single image size is 3.6 MB, and the original resolution is 1320 × 896. In our study, the experienced ophthalmologist performed the annotation of the cornea and tear meniscus to generate the ground truth masks. These masks were then overlaid onto the original images for evaluation purposes. Additionally, a second ophthalmologist reviewed the annotated images independently, and any areas of agreement between the two ophthalmologists were considered the final ground truth. This rigorous process involving multiple experts ensured the accuracy and reliability of the ground truth masks used in our study. We zoomed the authentic images and the corresponding labels to the size of 512 × 512. We split the data into 70% for training and 30% for testing. Data enhancement is a technique commonly used in deep learning to improve the generalization ability of models.[16] We performed data enhancement to obtain 3500 images, including the horizontal flip, vertical flip, affine transformation, rotation, Gaussian noise, horizontal flip + affine transformation, vertical flip + affine transformation, horizontal flip + Gaussian noise, vertical flip + Gaussian noise, and rotation + Gaussian noise. We used these data enhance-

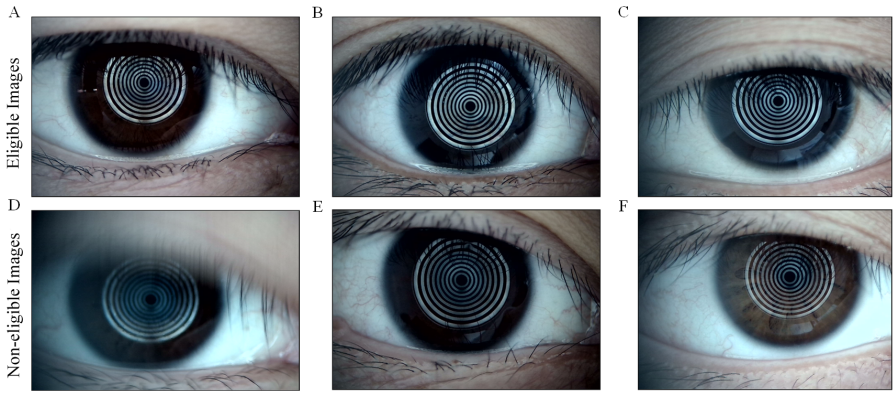

Figure 1. Eligible and non-eligible representative images for tear meniscus height analysis. (**A, B, C**) Represents the eligible images. (**D**) Indicates that the blur of the image may affect corneal recognition. (**E**) Indicates that the tear meniscus in the image is difficult to mark and may cause great visual errors. (**F**) Indicates that the light is too strong to observe the complete tear meniscus area.

Investigative Ophthalmology & Visual Science

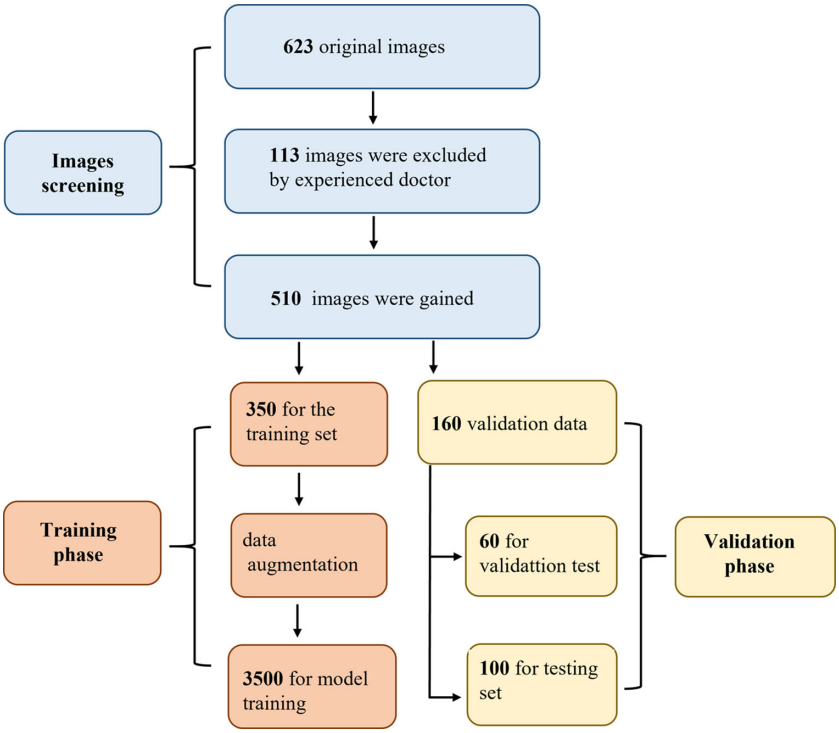

Figure 2. The flowchart demonstrates the dataset preprocessing procedure.

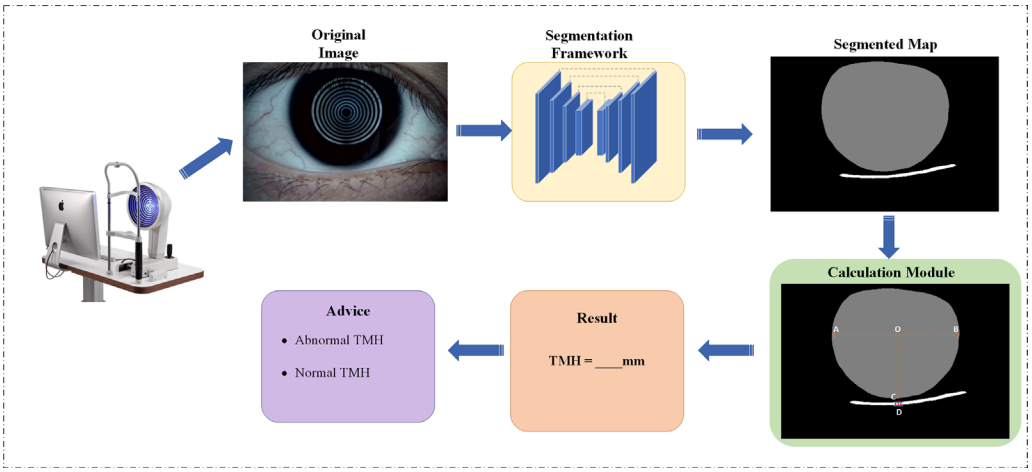

Figure 3. Whole system frame diagram for automatic quantitative assessment of the tear meniscus. TMH, tear meniscus height.

ment methods to prevent overfitting the neural network model, which improves the generalization of the AI system. The flowchart of the data preprocessing is described in Figure 2.

Establishment of the Automated Assessment System

In this study, the AI system for automatic evaluation of the tear meniscus includes the following 4 steps. (1) The original data and the corresponding mask are input into the neural network model. The constructed convoluted neural network model accurately segments the cornea and the tear meniscus region. (2) Calculating the number of pixels occupied by the maximum transverse diameter of the cornea. (3) Calculating the number of pixels occupied by the vertical distance between the upper and lower edges of the tear meniscus. (4) Calculating the TMH according to the geometric relationship between the cornea diameter and the pixel numbers. The whole workflow is depicted in Figure 3.

Development of Deep Learning Neural Network

To segment the cornea and the tear meniscus area, we construct a neural network model based on UNet. The UNet was first introduced into the segmentation of biomedical images in 2015 and has achieved good performance in many computer vision tasks.[17–19] In our work, we learned the idea that part of the convolution in the TransUNet[20] model is replaced by the Transformer, but considering that the Trans-

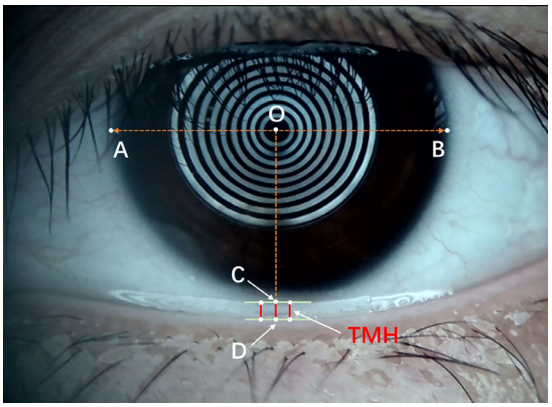

Figure 4. Schematic of calculation of tear meniscus height. TMH was calculated according to the formula in (1). (**A** and **B**) Representation of the left and right end points of the maximum transverse diameter of the cornea, respectively. (**C**) The *vertical line* intersects through the center of the cornea and the upper edge of the tear meniscus. (**D**) The corner of the vertical line passing through the center of the cornea and the lower edge of the tear meniscus. Line CD represents tear meniscus height (TMH). The *short red line* on the left and right of line CD are the line segments where line CD translates 10 pixels to the left and right of the intersection with the upper and lower edges of the tear meniscus, respectively. We calculated the average of these three as the final tear meniscus height.

former consumes a lot of resources during computation it does not apply to our work. Therefore, EficientNet was selected as an encoder in the contracting path instead of a conventional set of convolution layers. The decoder module is similar to the original UNet. Details of the proposed architecture are illustrated in Supplementary Figure S1. The basic building block of the EficientNet architecture is mobile inverted bottleneck convolution (MBConv). Each MBConvX block is shown with the corresponding filter size, and the X = 1 and X = 6 denote the standard ReLU and ReLU6 activation functions, respectively.

Calculation of Tear Meniscus Height

The average transverse diameter of the adult cornea (TDC) is approximately 11.5 mm.[21] We first used the deep-learning segmentation method (see Fig. 3) to obtain the mask map of the cornea region, and then we used digital image processing to obtain the coordinates of the left (A) and right end points (B) of the cornea, and their midpoint coordinates were O. Subsequently, based on point O, the coordinates of the intersection between the vertical line passing through point O and the upper and lower edges of the tear meniscus are represented by points C and D. The line CD represents the height of the tear meniscus. Hence, the pixels occupied by the transverse diameter of the cornea (P_{AB}) and the pixels occupied by the TMH (P_{CD}) were calculated. This study calculated the TMH according to the formula in Equation 1. The schematic of the calculation of TMH is demonstrated in Figure 4.

$$\text{TMH} = \frac{TDC * P_{CD}}{P_{AB}} \tag{1}$$

Model Evaluation

The Dice Similarity Coefficient (DSC) and Intersection over union (Iou) methods, which are widely used and reliable in the field of image segmentation,[22,23] were used to evaluate the performance of our modified model on visual tasks. DSC is often adopted to describe the degree of similarity of 2 samples with values between 0 and 1, the closer the value of DSC to 1 represents that the 2 samples are more similar. Iou is the other coincidence ratio used to describe the predicted target and the actual target area, and its value ranges from 0 to 1. In short, 1 indicates 100% coincidence between the expected region and the actual region, whereas 0 represents no coincidence region. Supplementary Figure S2 included a helpful diagram (left = DSC and right = Iou) to illustrate the meaning of these 2 metrics, making it easier to comprehend the model's performance.

To test our model's ability for distinguishing normal and abnormal TMH, the AI model's automatic measurement results with those of manual measurement by clinicians on the test were compared. All test data were reviewed to draw a binary confusion matrix. Additionally, accuracy (2), precision (3), sensitivity (4), specificity (5), and f1-score (6) were calculated, respectively.

$$\text{Accuracy} = \frac{TP + TN}{TP + TN + FP + FN} \tag{2}$$

$$\text{Precision} = \frac{TP}{TP + FP} \tag{3}$$

$$\text{Sensitivity} = \frac{TP}{TP + FN} \tag{4}$$

$$\text{Specificity} = \frac{TN}{TN + FP} \tag{5}$$

$$\text{F1 Score} = \frac{2 * Precision * Recall}{Precision + Recall} \tag{6}$$

TP, FN, FP, and TN present true positive, false negative, false positive, and true negative, respectively.

Furthermore, quantile-quantile(Q-Q) plots have been performed to test the normal distribution of the data.[24] The Bland-Altman plot[25] and the relatedness plot between the AI-predicted results and the physician's manual measurements were also presented to reveal the strength of the correlation between these two methods. Scatter curves were plotted by Matplotlib (version 3.5.3), Numpy (version 1.23.2), and Python (version 3.10.6).

Implement Details

The Pytorch deep learning framework and a 2080 GPU are used to perform model training. The loss function used is CrossEntropyLoss, with the optimizer being Adam. The initial learning rate is set at 0.005, and CosineAnnealingLR is utilized for adjustment. The batch size is set at 4, with the epoch of 100.

Results

Performance of Convolutional Neural Network

Based on the research plan presented in Figure 3, we leveraged labeled samples to conduct detailed experiments. In this experiment, we adopt a basic network model architecture UNet and 2 improved network model architectures, Effi-

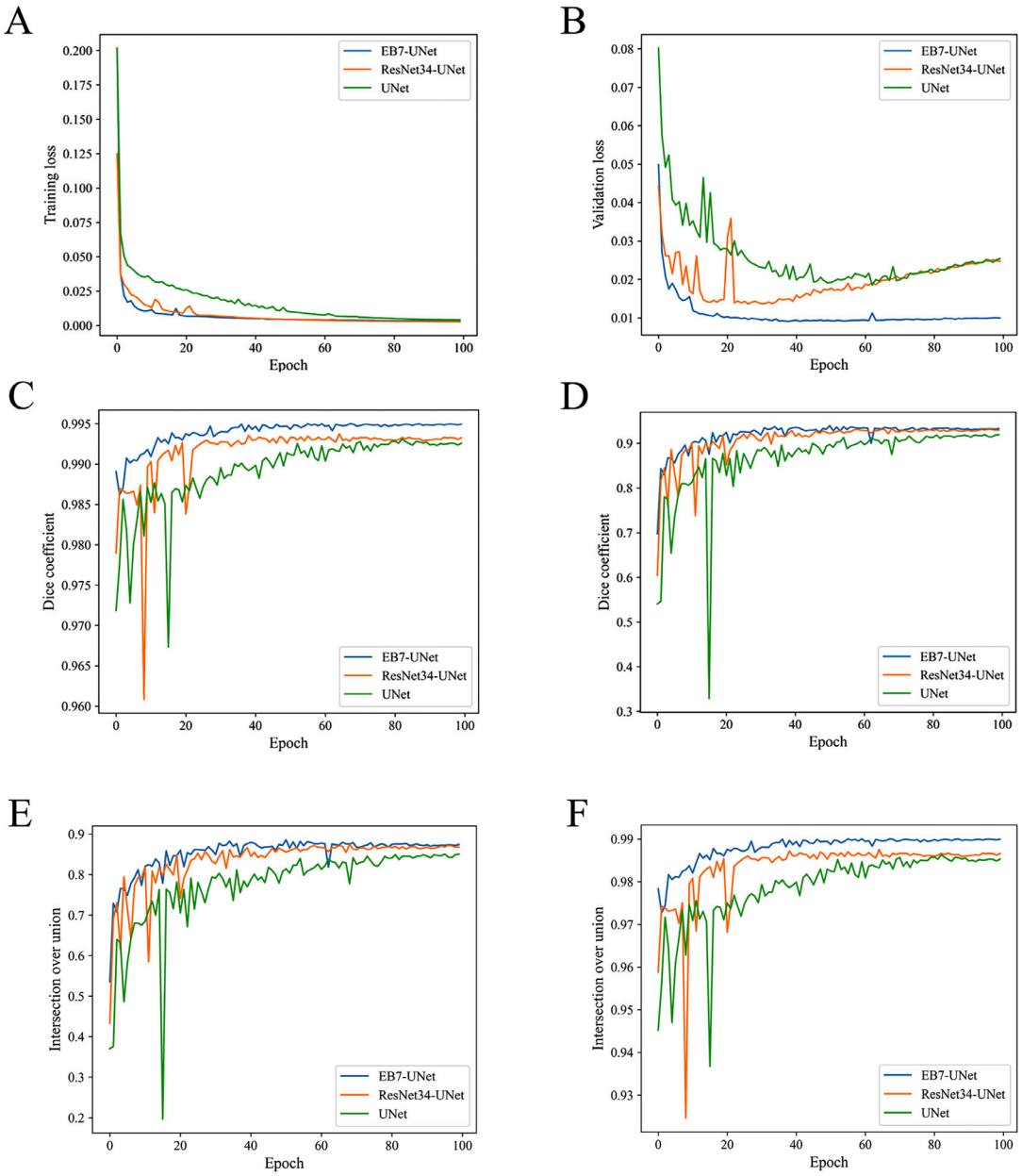

Figure 5. Quantitative evaluation of AI segmentation model. Training loss (**A**) and validation loss (**B**) of various neural network models. Dice coefficient of the cornea (**C**) and tear meniscus segmentation (**D**). Intersection over union (Iou) of the tear meniscus (**E**) and cornea (**F**) segmentation.

cientB7 encoded UNet (EB7-UNet), and ResNet34 encoded UNet (ResNet34-UNet) based on traditional UNet. Our modified model showed faster convergence in the training stage of the model compared with the classic UNet. The training loss of EB7-UNet and ResNet34-UNet reached the minimum at 20 epochs and remained stable during the subsequent training process, whereas the original UNet model did not reach the minimum until 80 epochs (Fig. 5A). In the validation stage, EB7-UNet first became the minimum value and remained stable at 20 training epochs, followed by ResNet34-UNet, and the slowest convergence was UNet. Compared with the speed of convergence of EB7-UNet, ResNet34-UNet, and UNet converges more slowly, and their minimum losses were also greater than the EB7-UNet model's (Fig. 5B).

Furthermore, to precisely evaluate the performance of these three models, we verified their ability to detect the boundary of the cornea and tear meniscus. The outcomes of our method in segmenting the cornea and the tear meniscus for both dice coefficient (Figs. 5C, 5D) and Iou (Figs. 5E, 5F) were depicted. As shown, the blue line representing EB7-UNet was corresponded to the largest value among all methods. More precisely, Supplementary Table S1 shows a specific comparison when our modified network converges. The DSC indexes of the cornea and tear meniscus reached 0.994556 and 0.937449, respectively, whereas those of Iou reached 0.989172 and 0.882263, respectively. The result of UNet is 0.25% and 2.54% lower than our method on the DSC index of the cornea and the tear meniscus, and 0.5%

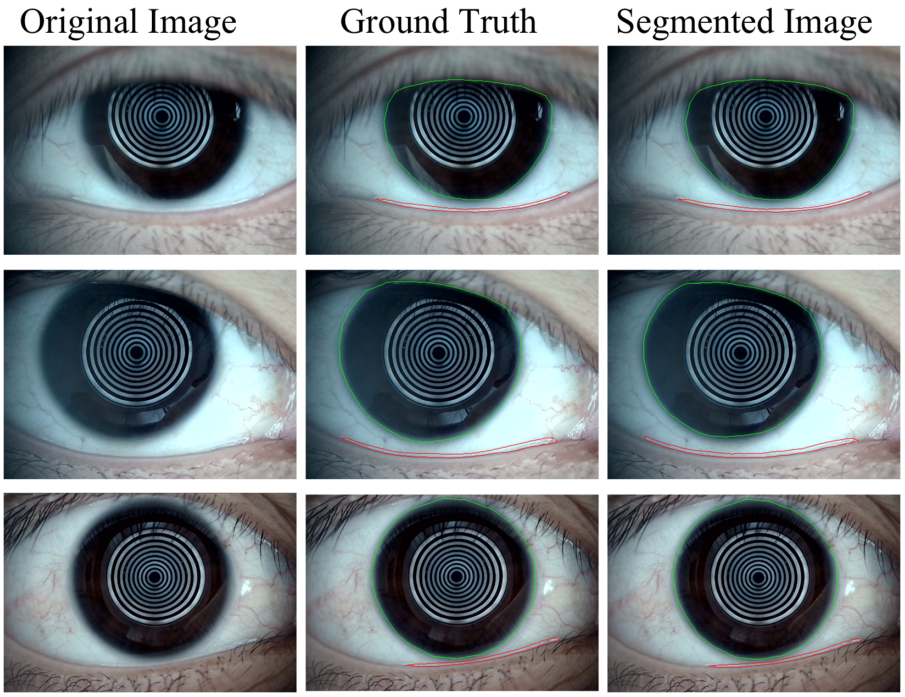

Figure 6. Representative images of corneal and tear meniscus segmentation. The original image, ground truth, and segmented image are from left to right; the closed areas surrounded by *red lines* represent the tear meniscus, and the *green lines* represent the cornea.

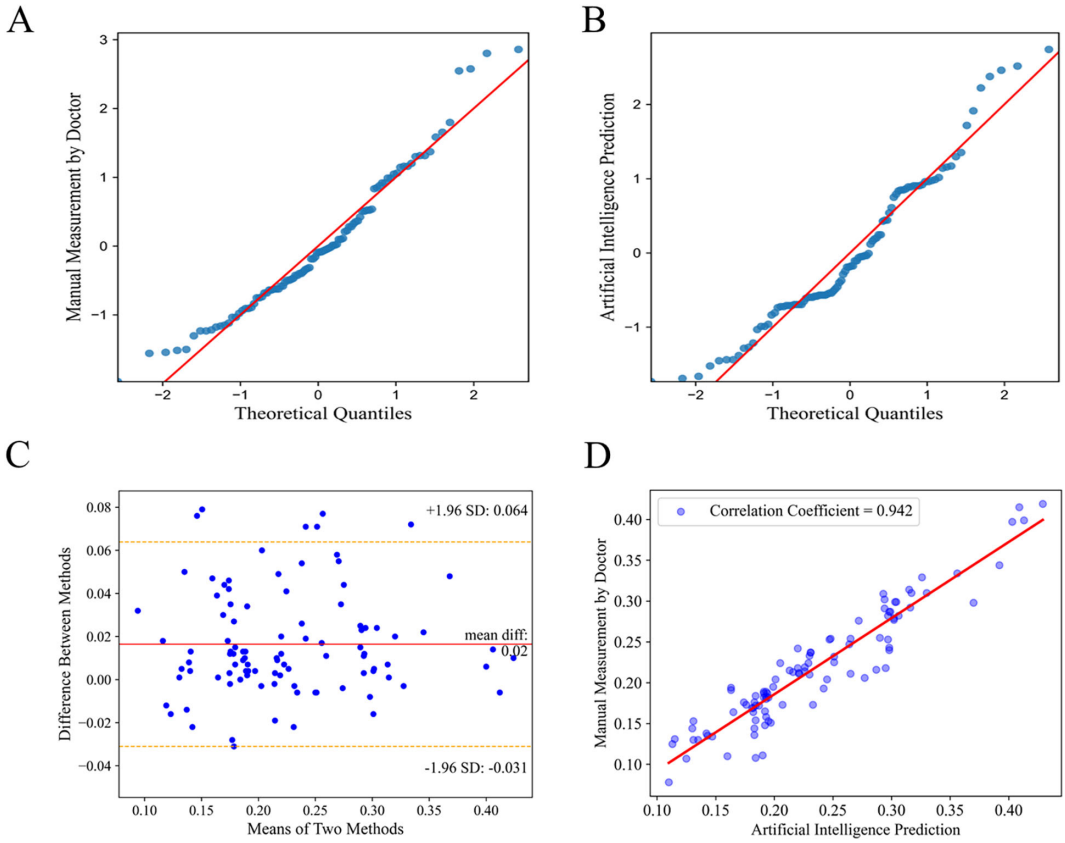

Figure 7. Comparison of AI prediction and ophthalmologist's manual measurement in the task of TMH measurement. The quantile-quantile (Q-Q) plot was used to perform a normal distribution test on data manually measured by ophthalmologists (**A**) and artificial intelligence prediction (**B**). Bland-Altman plot (**C**) was presented to describe the difference between the two methods. The upper and lower *dashed yellow lines* are 95% confidence intervals. (**D**) The graph shows the relation between AI prediction and manual measurement by a clinician. The *red line* is the regression line to fit the data (correlation coefficient = 0.942).

and 4.79% lower than our method on the Iou result. In comparison, ResNet34-UNet is 0.3% and 1.99% lower than our adapted way on the DSC index of the cornea and the tear meniscus, and 0.49% and 3.74% lower on the Iou indicator, respectively. In other words, our segmentation results are closer to the results labeled by ophthalmologists.

To observe the outcomes of AI model visually more intuitively, the EB7-UNet network was chosen to perform the visualization operation. We observed that there was no significant difference between the cornea and tear meniscus detected by our system and the standards labeled by experts (Fig. 6).

Comparison Between TMH of AI Prediction and the Clinicians

To further test the accuracy of our AI system in measuring the TMH, we compared the results automatically predicted by the AI system with the results manually measured by the ophthalmologist. First, normality tests were performed manually on data measured manually by ophthalmologists (Fig. 7A) and automatically reported by AI systems (Fig. 7B). Both data sets were shown to follow a normal distribution.

The results showed that most data were within the 95% confidence interval, and only 6 points fell outside the boundaries (Fig. 7C). Furthermore, we plotted the relatedness result between the 2 methods, showing that the correlation coefficient between these 2 ways was 0.942 (Fig. 7D), indicating that the intelligent system is strongly correlated with the results manually measured by the ophthalmologists.

It is well-known that TMH < 0.2 mm is the criterion for diagnosing dry eye. TMH < 0.2 mm is here recorded as abnormal.[26] To comprehensively determine the recognition ability of our AI system at normal as well as abnormal TMH, we showed the performance of the AI system in binary classification on the test set. Supplementary Table S2 presents the confusion matrix consisting of AI prediction and manual measurement by an ophthalmologist. As shown in Supplementary Table S3, our developed model achieved better results with 96% accuracy, 93.1% precision, 100% sensitivity, 91.3% specificity, and 96.4% f1-score, respectively.

Discussion

In this study, we constructed an AI system to measure the TMH automatically. Using Oculus photographs, our modified method performed excellently in identifying the tear meniscus, reaching 0.937449 and 0.882263 for DSC and Iou, respectively. Subsequently, we utilized the distinct physical attributes of the human anatomy in a resourceful manner to calculate the height of the tear meniscus. This system will display the segmented map and the calculated height of the tear meniscus. Furthermore, it can automatically determine whether the TMH is within the normal range. The acquisition of these results does not require manual intervention and has shown a correlation with measurements conducted by ophthalmologists. These results provide reliable qualitative and quantitative references for clinical diagnosis.

Quantitative assessment of the tear meniscus is essential for diagnosing dry eye. However, almost all quantitative assessments rely on manual measurement by clinicians. Because of the influence of factors, such as operator technique and non-uniform clinical measurement methods, there is no effective, simple, and rapid method to evaluate the tear meniscus so far. An automatic screen tool developed in this study could be applied in the hospital, which has great potential to diagnose dry eye in the early stage.

It is undeniable that there are still some drawbacks in our study. First, our AI system uses Oculus keratographs taken with professional hospital equipment. A single photograph input source may limit the application scenario of the AI system. Slit lamp photographs and photographs taken with intelligent devices, such as smartphones, are currently unable to accurately show the boundary range of the tear meniscus, a direction worth further work in the future. Second, we select the mean value of TMH in this experiment at three locations as the measurement result. Although it can somewhat alleviate the measurement error, we believe that the area of the entire tear meniscus range identified by this system can be used as a biomarker reflecting tear storage in the future for more in-depth study. Finally, the results of this study remain to be tested in large-scale clinical work.

In conclusion, we propose a fully automated AI system for quantifying tear meniscus. Our experimental results showed that this system could accurately identify the tear meniscus region. Additionally, the measurement outcomes of TMH through this AI system can be finished automatically without human intervention. As an effective screen tool, this AI system has the potential to be leveraged on keratographs for diagnosing dry eye in the early stage.

Acknowledgments

Supported by the National Natural Science Foundation of China (No. 82271054, ZL; No. 82201149, XH). The funders have no role in the study design, data collection and analysis, decision on publishing, or manuscript preparation.

Availability of Data and Materials: Data and related materials used in this study are available upon reasonable request from the corresponding author.

Disclosure: **S. Wang**, None; **X. He**, None; **J. He**, None; **S. Li**, None; **Y. Chen**, None; **C. Xu**, None; **X. Lin**, None; **J. Kang**, None; **W. Li**, None; **Z. Luo**, None; **Z. Liu**, None

References

1. Craig JP, Nichols KK, Akpek EK, et al. TFOS DEWS II Definition and Classification Report. *Ocul Surf*. 2017;15:276–283.
2. Stapleton F, Alves M, Bunya VY, et al. TFOS DEWS II Epidemiology Report. *Ocul Surf*. 2017;15:334–365.
3. Rouen PA, White ML. Dry eye disease: prevalence, assessment, and management. *Home Healthc Now*. 2018;36:74–83.
4. Yamada M, Mizuno Y, Shigeyasu C. Impact of dry eye on work productivity. *Clinicoecon Outcomes Res*. 2012;4:307–312.
5. Wolffsohn JS, Arita R, Chalmers R, et al. TFOS DEWS II diagnostic methodology report. *Ocul Surf*. 2017;15:539–574.
6. Wei A, Le Q, Hong J, Wang W, Wang F, Xu J. Assessment of lower tear meniscus. *Optom Vis Sci*. 2016;93:1420–1425.
7. Shen D, Wu G, Suk HI. Deep learning in medical image analysis. *Annu Rev Biomed Eng*. 2017;19:221–248.
8. Li Z, Jiang J, Chen K, et al. Preventing corneal blindness caused by keratitis using artificial intelligence. *Nat Commun*. 2021;12:3738.
9. Li F, Su Y, Lin F, et al. A deep-learning system predicts glaucoma incidence and progression using retinal photographs. *J Clin Invest*. 2022;132:e157968.

10. Long E, Lin H, Liu Z, et al. An artificial intelligence platform for the multihospital collaborative management of congenital cataracts. *Nat Biomed Eng*. 2017;1:0024.
11. Poplin R, Varadarajan AV, Blumer K, et al. Prediction of cardiovascular risk factors from retinal fundus photographs via deep learning. *Nat Biomed Eng*. 2018;2:158–164.
12. Stegmann H, Werkmeister RM, Pfister M, Garhofer G, Schmetterer L, Dos Santos VA. Deep learning segmentation for optical coherence tomography measurements of the lower tear meniscus. *Biomed Opt Express* .2020;11:1539–1554.
13. Gabriele ML, Wollstein G, Ishikawa H, et al. Three dimensional optical coherence tomography imaging: advantages and advances[J]. *Prog Retin Eye Res*, 2010, 29(6):556–579.
14. Tittler EH, Bujak MC, Nguyen P, et al. Between-grader repeatability of tear meniscus measurements using Fourier-domain OCT in patients with dry eye. *Ophthalmic Surg Lasers Imaging*. 2011;42:423–427.
15. Wan C, Hua R, Guo P, et al. Measurement method of tear meniscus height based on deep learning. *Front Med*. 2023;10:1126754.
16. Shorten C, Khoshgoftaar TM. A survey on image data augmentation for deep learning. *J Big Data*. 2019;6:1–48.
17. Ronneberger O, Fischer P, U-Net Brox T.: *Convolutional networks for biomedical image segmentation. International Conference on Medical Image Computing and Computer-Assisted Intervention*. New York, NY: Springer; 2015:234–241.
18. Xiao X, Lian S, Luo Z, Li S. Weighted res-unet for high-quality retina vessel segmentation. *2018 9th International Conference on Information Technology in Medicine and Education (ITME)*. Piscataway, NJ: IEEE; 2018:327–331.
19. Hu X, Naiel MA, Wong A, Lamm M, Fieguth P. RUNet: a robust UNet architecture for image super-resolution. *Proceedings of the IEEE/CVF Conference on Computer Vision and Pattern Recognition Workshops*; 2019:0–0.
20. Chen J, Lu Y, Yu Q, et al. TransUNet: Transformers make strong encoders for medical image segmentation. *arXiv preprint arXiv:210204306* 2021.
21. Sanchis-Gimeno JA, Sanchez-Zuriaga D, Martinez-Soriano F. White-to-white corneal diameter, pupil diameter, central corneal thickness and thinnest corneal thickness values of emmetropic subjects. *Surg Radiol Anat*. 2012;34:167–170.
22. Guindon B, Zhang Y. Application of the Dice Coefficient to accuracy assessment of object-based image classification. *Can J Remote Sens*. 2017;43:48–61.
23. Rahman MA, Wang Y. Optimizing intersection-over-union in deep neural networks for image segmentation. *International Symposium on Visual Computing*. New York, NY: Springer; 2016:234–244.
24. Das KR, Rahmatullah Imon AHM. A brief review of tests for normality. *Am J Theoretic Applied Stat*. 2016;5:5–12.
25. Giavarina DJBM. Understanding Bland Altman analysis. *Biochem Med (Zagreb)*. 2015;25:141–151.
26. Safarzadeh M, Safavi M, Azizzadeh P, Akbarshahi P. Assessment of non-invasive tear break-up time and tear meniscus height after instillation of three different formulations of anesthetic eye drops by Oculus Keratograph 5M. *Revista Brasileira de Oftalmologia*. 2018;77:244–247.

Investigative Ophthalmology & Visual Science